The Astronomical Journal, 153:274 (7pp), 2017 June https://doi.org/10.3847/1538-3881/aa7139

Isotopic Evidence for Multi-stage Cosmic-ray Exposure Histories of Lunar Meteorites: Long Residence on the Moon and Short Transition to the Earth

Hiroshi Hidaka[1,2], Keisuke Sakuma[1,2], Kunihiko Nishiizumi[3], and Shigekazu Yoneda[4]
[1] Department of Earth and Planetary Sciences, Nagoya University Nagoya 464-8601, Japan; hidaka@eps.nagoya-u.ac.jp
[2] Department of Earth and Planetary Systems Science, Hiroshima University Higashi-Hiroshima 739-8526, Japan
[3] Space Sciences Laboratory, University of California, Berkeley, CA 94720-7450, USA
[4] Department of Science and Engineering, National Museum of Nature and Science Tsukuba 305-0005, Japan
Received 2017 March 11; revised 2017 April 30; accepted 2017 May 2; published 2017 June 2

Abstract

It is known that most lunar meteorites have complicated cosmic-ray exposure experiences on the Moon and in space. In this study, cosmic-ray irradiation histories of six lunar meteorites, Dhofar 489, Northwest Africa 032 (NWA 032), NWA 479, NWA 482, NWA 2995, and NWA 5000, were characterized from neutron-captured isotopic shifts of Sm and Gd, and from the abundances of long-lived cosmogenic radionuclides like ^{10}Be, ^{26}Al, ^{36}Cl, and ^{41}Ca. Sm and Gd isotopic data of all of six meteorites show significant isotopic shifts of ^{149}Sm–^{150}Sm and ^{157}Gd–^{158}Gd caused by accumulation of neutron capture reactions due to cosmic-ray irradiation, corresponding to the neutron fluences of (1.3–9.6) $\times$ 10^{16} n cm^{-2}. In particular, very large Sm and Gd isotopic shifts of NWA 482 are over those of a lunar regolith 70002, having the largest isotopic shifts among the Apollo regolith samples, corresponding to cosmic-ray exposure duration over 800 million years in the lunar surface (2π irradiation). Meanwhile, the concentrations of cosmogenic radionuclides for individual six meteorites show the short irradiation time less than one million years as their bodies in space (4π irradiation). Our data also support the results of previous studies, revealing that most of lunar meteorites have long exposure ages at shallow depths on the Moon and short transit times from the Moon to the Earth.

Key words: meteorites, meteors, meteoroids – Moon

1. Introduction

The analyses of lunar materials returned by the Apollo and Luna missions provide valuable information to understand the evolution processes of the Moon. However, the returned materials were collected from the restricted areas at low latitude nearside localities on the Moon, and do not fully cover the comprehensive view about the geological diversity of the whole Moon. The importance of the characterization of lunar meteorites is that the individual samples were derived from random regions on the global sample-set of lunar surface. Mineralogical, petrological, geochemical, and isotopic studies of lunar meteorites are expected to offer new and additional information on the lunar mantle evolution that has not been known from the Apollo and Luna missions samples (Korotev 2005; Joy & Arai 2013).

Most lunar meteorites have complicated cosmic-ray exposure histories with relatively longer exposure times than the other stony meteorites, although it has been generally known from the analyses of the cosmogenic radionuclides that their transfer times from Moon to Earth are generally quite short (Nishiizumi et al. 1996). Isotopic compositions of Sm and Gd can be used to characterize exposure history of the samples from isotopic shifts of ^{149}Sm–^{150}Sm and ^{157}Gd–^{158}Gd due to neutron capture effect, because lunar meteorites have more or less been affected by contribution of cosmic-ray irradiation on the Moon (Hidaka & Yoneda 2013; Welten et al. 2013). A combination of the measurements of cosmogenic radionuclides with Sm and Gd isotopic shifts in individual lunar meteorites provides an estimation of the exposure durations on the Moon and in space. Detailed exposure histories of lunar meteorites can be applied for the construction of impact and ejection mechanisms.

In this study, we collected systematic data sets of neutron-captured Sm and Gd isotopes and long-lived cosmogenic radionuclides of six lunar meteorites, Dhofar 489, Northwest Africa (hereafter NWA) 032, NWA 479, NWA 482, NWA 2995, and NWA 5000 to investigate the details of the exposure histories of individual meteorites.

2. Experimental Methods

2.1. Samples

Six lunar meteorites, Dhofar 489, NWA 032, NWA 479, NWA 482, NWA 2995, and NWA 5000, were used in this study. Dhofar 489 is a crystalline matrix anorthositic breccia. The idea that Dhofar 489 is from the farside highlands of the Moon because of the mineralogical and chemical aspects like feldspathic composition and low concentration of Th and Fe in the meteorite is suggested by Takeda et al. (2007). However, the results by the Clementine and Lunar Prospector missions show that low-Fe and low-Th regions like Dhofar 489 exist not only on the farside but also on the nearside (Korotev et al. 2006). The origin of Dhofar 489 is still unclear and disputable.

NWA 032 is an unbrecciated mare basalt and is considered to be a pair with NWA 479. The crystallization ages of 2.95 Ga, 2.93 Ga, and 2.72 Ga are given by Rb–Sr, Sm–Nd (Borg et al. 2009), and ^{40}Ar–^{39}Ar data (Fernandes et al. 2009), respectively, which are known as the youngest lunar basaltic meteorites.

NWA 482 is a crystalline impact-melt polymict breccia with highland affinities. Late impact events after the crystallization may provide the disagreement of its chronometric results between different isotopic systems such as K–Ar, Ar–Ar, and Sm–Nd. The most plausible scenario of NWA 482 is that the original crystallization age is 4.4–4.5 Ga, the formation of the

impact-melt breccia occurred <3750 Ma, and the launching time from Moon to Earth is 9 Ka (Daubar et al. 2002).

NWA 2995 is a feldspathic breccia containing mare lithologies (Carpenter et al. 2017). From the mineralogical and chemical similarities of the bulk composition, it has been paired with other five specimens, NWA 2996, 3190, 4503, 5151, and 5152 (Connolly et al. 2008; Weisberg et al. 2008, 2009). The origin of one of the six, NWA 2996, is suggested as the South Pole Aitken (Mercer et al. 2013).

NWA 5000, known as one of the largest lunar meteorites having 11.5 kg of recovery mass, is a feldspathic monomict breccia including Mg-suite olivine gabbro clasts. The ^{40}Ar–^{39}Ar age spectra suggest a large impact age of 3.2 Ga and a partial resetting of the K/Ar system around 500 Ma (Fernandes et al. 2009). The data of a series of cosmogenic nuclides provide the individual exposure histories of a long residence in the lunar regolith and a short transition time from the Moon to Earth (Nishiizumi et al. 2009).

2.2. Sm and Gd Isotopic Measurements

Prior to chemical procedure, each sample was washed twice with 0.2 M HNO_3 in an ultrasonic bath for 10 minutes in order to eliminate terrestrial contaminants. Individual powderized samples weighing 40–70 mg were completely decomposed by HF+$HClO_4$, and were finally redissolved in 1 mL of 2 M HCl. The solutions were divided into two portions: the main portion for isotopic measurements by thermal ionization mass spectrometry and the rest for the determination of elemental abundances of rare earth elements (REE) by inductively coupled plasma mass spectrometry (ICP-MS).

Most of the sample solution was used for the Sm and Gd isotopic measurements. As the first step, each solution was loaded onto a cation exchange resin packed column (Bio-Rad AG50WX8, 200–400 mesh, H^+ form, 50 mm length × 4.0 mm diameter). The column was washed with 3.2 mL of 2 M HCl, and was washed with 4.5 mL of 6 M HCl to recover the REE elution. The solution was then evaporated to dryness and redissolved in a drop of 0.1 M HCl. The REE fraction was loaded onto a second column packed with lanthanide-specific resin (Eichrom, LN resin, particle size of 100–150 μm, 100 mm length × 2.5 mm diameter) to separate Sm and Gd using 0.25, 0.35, and 0.5 M HCl, respectively (Hidaka & Yoneda 2007).

The Japanese National Museum of Nature and Science moved from Tokyo to Tsukuba in 2011 September, and a new thermal ionization mass spectrometer, Triton Plus, has been installed since the end of 2011. Before then, VG Sector54-30 was used for the isotopic work. The isotopic analyses of two of six samples treated in this study, Dhofar 489 and NWA 032, were performed by the VG Sector54-30 equipped with seven Faraday cup collectors, and those of the other four samples were done by Triton Plus with nine Faraday cup collectors.

Sm and Gd were measured on double Re filaments. For their isotopic measurements, $^{147}Sm/^{152}Sm = 0.56081$ and $^{156}Gd/^{160}Gd = 0.9361$ were used to correct for instrumental mass fractionation using the exponential law. When the isotopic depletions of ^{155}Gd were found in the analyses, the Gd isotopic data sets were normalized by $(^{155}Gd+^{156}Gd)/^{160}Gd = 1.61290$ (Hidaka et al. 1995). The details for mass spectrometric techniques were given in our previous references (by VG Sector54-30; Hidaka & Yoneda 2007; by Triton Plus; Hidaka & Yoneda 2014). The isotopic data of Sm and Gd of six samples are listed in Table 1.

Another minor aliquot of each sample solution except for Dhofar 489 and NWA 032 was used for the determination of REE contents. In this study, Dhofar 489 and NWA 032 were used only for isotopic works, because their absolute amounts were limited. The solution was once evaporated to dryness, and redissolved using 5 mL of 0.5 M HNO_3. A 0.05 g quantity of a 1 ppb indium solution was added to the individual sample solutions as an internal standard element to optimize the analytical conditions for REE measurements. An ICP-MS (Agilent 7500cx) was used for the analyses. The data of REE concentrations of the samples are given in Table 2.

2.3. AMS Analyses of Short-lived Radionuclides, ^{10}Be, ^{26}Al, and ^{36}Cl

Each sample was crushed and dissolved with a HF-HNO_3 mixture, together with Be, Al, and Cl carriers. A small aliquot of the sample solution was used for the determination of the concentration of major target elements Mg, Al, K, Ca, Mn, and Fe by atomic absorption spectrometry. The data are listed in Table 3. Another aliquot of the solution was used for the chemical separation of Be, Al, and Cl, using a combination of ion chromatographic and liquid–liquid extraction techniques (Nishiizumi et al. 1984a, 1984b). The concentration of ^{10}Be, ^{26}Al, and ^{36}Cl were measured using accelerator mass spectrometry (AMS) at the Lawrence Livermore National Laboratory.

The data of short-lived cosmogenic radionuclides were partly reported before (e.g., Nishiizumi & Caffee 2001; Welten et al. 2001; Nishiizumi et al. 2004, 2009). In this paper, for further discussion, we have compiled additional data with previously reported data for the abundances of cosmogenic radionuclides and estimated 2π and 4π exposure ages shown in Table 4 and a part of Table 5, respectively.

3. Results and Discussion

3.1. Sm and Gd Isotopic Shifts due to Neutron Capture Effects

Significant exposure records of some lunar meteorites in the lunar regolith are suggested for their long CRE ages, in spite of very short transfer duration from the Moon to the Earth (Nishiizumi et al. 1996; Welten et al. 2013). Sm and Gd isotopic shifts are useful tracers to recognize the accumulation of CRE records, because their isotopic shifts from ^{149}Sm to ^{150}Sm and from ^{157}Gd to ^{158}Gd by neutron capture reaction of (n, γ) type are given by variations of stable isotopes in a single element. Figure 1 shows three-isotope plot diagrams for $^{149}Sm/^{152}Sm$ versus $^{150}Sm/^{152}Sm$ and $^{157}Gd/^{160}Gd$ versus $^{158}Gd/^{160}Gd$, which are effectively used to understand the magnification of neutron capture reactions for individual samples. In the case of (n, γ) type-neutron capture reactions, the decrements of ^{149}Sm and ^{157}Gd isotopic abundances quantitatively correspond to the increments of ^{150}Sm and ^{158}Gd isotopic abundances, respectively. As the results, the data points of the samples affected by neutron capture reactions should be ideally plotted on the line with a slope of −1 in the diagrams. All data points from the six samples are plotted on the line both in the Sm and Gd diagrams, showing clear evidence for the occurrence of neutron capture reactions. A wide variation of the Sm and Gd isotopic shifts observed in six data points suggests a difference of exposure condition of cosmic rays, like a duration and a shielding depth. Sm and Gd isotopic

Table 1
Sm and Gd Isotopic Compositions of the Lunar Meteorites Used in This Study

(a) Isotopic Compositions of Sm

Sample	$^{144}Sm/^{152}Sm$	$^{148}Sm/^{152}Sm$	$^{149}Sm/^{152}Sm$	$^{150}Sm/^{152}Sm$	$^{154}Sm/^{152}Sm$
STD	01149744 ± 4	0.4204410 ± 5	0.516872 ± 4	0.275995 ± 3	0.850854 ± 7
Lunar meteorite Dhofar 489		0.420434 ± 18	0.516731 ± 20	0.276123 ± 24	0.850882 ± 43
NWA 032		0.420463 ± 17	0.516282 ± 18	0.276619 ± 14	0.850845 ± 30
NWA 479	01149774 ± 6	0.4204550 ± 8	0.5162191 ± 8	0.2766339 ± 6	0.8507813 ± 16
NWA 482	01149782 ± 9	0.4204392 ± 13	0.5130974 ± 35	0.2793920 ± 27	0.8507788 ± 67
NWA 2995	01149783 ± 9	0.4204398 ± 13	0.5138094 ± 14	0.2790255 ± 9	0.8507802 ± 25
NWA 5000	01149763 ± 19	0.4204366 ± 22	0.5149839 ± 23	0.2777814 ± 18	0.8507496 ± 41

(b) Isotopic compositions of Gd

Sample	$^{152}Gd/^{160}Gd$	$^{154}Gd/^{160}Gd$	$^{157}Gd/^{160}Gd$	$^{158}Gd/^{160}Gd$
STD	0.009259 ± 1	0.099695 ± 1	0.715878 ± 4	1.135846 ± 7
Lunarmeteorite Dhofar 489	No data	No data	0.715578 ± 61	1.136141 ± 51
NWA 032	No data	No data	0.714533 ± 49	1.137146 ± 53
NWA 479	0.009260 ± 18	0.099717 ± 20	0.714554 ± 74	1.137029 ± 48
NWA 482	0.009290 ± 14	0.099791 ± 13	0.707269 ± 96	1.144310 ± 97
NWA 2995	0.009279 ± 18	0.099788 ± 23	0.710062 ± 32	1.141545 ± 41
NWA 5000	0.009270 ± 15	0.099689 ± 12	0.711966 ± 64	1.139615 ± 56

Note. (a) Errors are 2σ of mean. All of the data are normalized to $^{147}Sm/^{152}Sm = 0.56081$. (b) Errors are 2σ of mean. All of the data are normalized to $(^{155}Gd + {}^{156}Gd)/^{160}Gd = 1.61290$.

Table 2
REE Concentration (ppm) of the Lunar Meteorites Used in This Study

	NWA 479	NWA 482	NWA 2995	NWA 5000
La	13.1 ± 0. 1	1.07 ± 0.01	10.7 ± 0.1	3.77 ± 0.02
Ce	34.4 ± 0.02	2.73 ± 0.02	27.2 ± 0.2	9.32 ± 0.05
Pr	5.07 ± 0.09	0.381 ± .003	3.83 ± 0.03	1.34 ± 0.01
Nd	23.6 ± 0.2	1.66 ± 0.02	16.6 ± 0.2	5.84 ± 0.17
Sm	7.62 ± 0.04	0.488 ± 0.002	4.73 ± 0.03	1.62 ± 0.01
Eu	1.39 ± 0.01	0.558 ± 0.006	1.09 ± 0.01	0.877 ± 0.8
Gd	9.77 ± 0.05	0.588 ± 0.003	5.47 ± 0.05	1.90 ± 0.02
Tb	1.88 ± 0.02	0.113 ± 0.02	1.00 ± 0.01	0.352 ± 0.04
Dy	1.39 ± 0.08	0.817 ± 0.0191	7.06 ± 0.06	2.50 ± 0.03
Ho	3.06 ± 0.02	0.182 ± 0.02	1.53 ± 0.01	0.544 ± 0.03
Er	8.66 ± 0.02	0.526 ± 0.007	4.29 ± 0.06	1.54 ± 0.01
Tm	1.27 ± 0.01	0.0783 ± 0.0022	0.621 ± 0.061	0.225 ± 0.001
Yb	7.84 ± 0.049	0.492 ± 0.003	3.82 ± 0.03	14.0 ± 0.01
Lu	1.16 ± 0.01	0.0736 ± 0.006	0.553 ± 0.005	0.205 ± 0.002

Note. Analytical errors are shown in 1σ of the means.

Table 3
Elemental Concentrations of Mg, Al, K, Ca, Mn, Fe, Co, and Ni of the Lunar Meteorites Used in This Study

Sample	Mg (%)	Al (%)	K (ppm)	Ca (%)	Mn (ppm)	Fe (%)	Co (ppm)	Ni (ppm)
Dhofar 489 (0–2 mm)	3.86	13.71	240	11.74	460	2.86	20	40
Dhofar 489 (interior)	3.48	15.27	130	12.32	290	2.20	20	30
NWA 032 (A) (0–1.5 mm)	4.18	4.16	850	8.22	2100	15.78	80	40
NWA 032 (A) (interior)	4.30	4.05	830	7.81	2090	15.83	80	40
NWA 032 (B) (0–2 mm)	4.08	5.07	950	7.53	2100	16.05	80	40
NWA 482 (A) (0–1 mm)	2.61	13.90	960	10.48	390	3.06	20	170
NWA 482 (A) (1–2 mm)	2.34	14.90	690	10.48	350	3.05	20	150
NWA 482 (A) (7–8.5 mm)	2.38	15.74	390	12.58	350	2.79	20	120
NWA 482 (B) (0–1.5 mm)	2.56	15.42	360	13.14	440	2.97	20	130
NWA 482 (B) (10–12 mm)	2.39	15.01	290	12.21	410	3.04	20	140
NWA 2995 (0–1.5 mm)	4.88	11.26	1330	9.17	940	7.94	50	170
NWA 2995 (1.5–5 mm)	4.77	11.51	1250	9.00	870	7.64	50	180
NWA 5000	4.76	12.8	430	9.93	620	5.19	30	220

Table 4
Abundances of Cosmogenic Radionuclides (dpm kg^{-1}) and Estimated Burial Depth (g cm^{-2}) of the Lunar Meteorites Used in This Study

Sample	^{10}Be	^{26}Al	^{36}Cl	^{36}Cl[a]	^{41}Ca	Burial Depth
Dhofar 489 (0–2 mm)	0.071 ± 0.013	0.352 ± 0.043	0.122 ± 0.009	0.125 ± 0.009	1.0 ± 0.5	>1100
Dhofar 489 (interior)	0.041 ± 0.013	0.381 ± 0.105	0.076 ± 0.005	0.076 ± 0.005	0.2 ± 0.3	
NWA 032 (A) (0–1.5 mm)	0.400 ± 0.105	4.42 ± 0.33	1.389 ± 0.045	1.379 ± 0.044	3.2 ± 2.7	>1100
NWA 032 (A) (interior)	0.318 ± 0.066	2.94 ± 0.26	1.303 ± 0.040	1.349 ± 0.041	2.8 ± 1.4	
NWA 032 (B) (0–2 mm)	0.285 ± 0.012	4.48 ± 0.21	1.270 ± 0.054	1.631 ± 0.070	n.d.	
NWA 482 (A) (0–1 mm)	6.00 ± 0.10	80.8 ± 3.8	10.60 ± 0.23	9.56 ± 0.21	23.8 ± 3.2	240
NWA 482 (A) (1–2 mm)	5.87 ± 0.09	79.7 ± 2.0	11.62 ± 0.31	10.56 ± 0.28	29.0 ± 3.4	
NWA 482 (A) (7–8.5 mm)	6.31 ± 0.10	70.3 ± 1.8	12.37 ± 0.23	9.53 ± 0.18	29.1 ± 2.2	
NWA 482 (B) (0–1.5 mm)	6.60 ± 0.10	64.7 ± 2.6	11.70 ± 0.23	8.63 ± 0.17	32.3 ± 2.0	
NWA 482 (B) (10–12 mm)	6.36 ± 0.10	58.7 ± 1.5	12.62 ± 0.34	10.01 ± 0.27	27.8 ± 2.1	
NWA 2995 (0–1.5 mm)	5.28 ± 0.19	33.8 ± 1.4	8.55 ± 0.16	10.25 ± 0.20	n.d.	230
NWA 2995 (1.5–5 mm)	5.33 ± 0.21	32.7 ± 1.1	8.36 ± 0.14	10.24 ± 0.18	n.d.	
NWA 5000	2.93 ± 0.03	16.6 ± 0.08	3.94 ± 0.14	4.61 ± 0.16	n.d.	335

Notes. n.d.: no determination.
[a] dpm ^{36}Cl/kg (Fe+8Ca+16K).

Table 5
Summary of Parameters to Characterize Neutron Capture Reactions and CRE Ages of the Lunar Meteorites Used in This Study

Sample	^{150}Sm/^{149}Sm	^{158}Gd/^{157}Gd	$\varepsilon_{Sm}/\varepsilon_{Gd}$	Ψ (1016 n cm^{-2})	σ_{eff} (cm^2 g^{-1})	CRE Age	
						4π Exposure	2π Exposure
STD	0.533991 ± 6	1.58667 ± 1	…	…	…	…	…
Dhofar 489	0.534365 ± 51	1.58772 ± 13	0.616 ± 0.089	0.457 ± 0.075	0.0031	6 Ka (1)	No data
NWA 032	0.536088 ± 33	1.59145 ± 16	0.743 ± 0.032	2.24 ± 0.07	0.0097	0.042 Ma (2)	212-275 Ma (3)
NWA 479	0.535885 ± 1	1.59124 ± 2	0.702 ± 0.003	2.34 ± 0.01	0.0097	0.042 Ma (2)	275 Ma (4)
NWA 482	0.544520 ± 6	1.62030 ± 2	0.532 ± 0.003	12.6 ± 0.01	0.0032	0.9 Ma (5)	800 Ma
NWA 2995	0.543053 ± 2	1.61080 ± 1	0.636 ± 0.006	11.1 ± 0.01	0.0055	<1 Ma	680 Ma
NWA 5000	0.539398 ± 4	1.60066 ± 2	0.654 ± 0.002	6.61 ± 0.01	0.0041	1.3 Ka (6)	550 Ma

Note. Numbers as analytical errors of ^{150}Sm/^{149}Sm and ^{158}Gd/^{157}Gd are 2σ of the means of the last digits indicated. $\varepsilon_{Sm}/\varepsilon_{Gd}$: a parameter for neutron energy spectrum (see text). Ψ: neutron fluences estimated from ^{150}Sm/^{149}Sm given by the equation as shown in the text. The data of CRE ages are from (1) Nishiizumi et al. (2004), (2) Welten et al. (2001), (3) Elardo et al. (2014), (4) Fernandes et al. (2009), (5) Nishiizumi & Caffee (2001), (6) Nishiizumi et al. (2009).

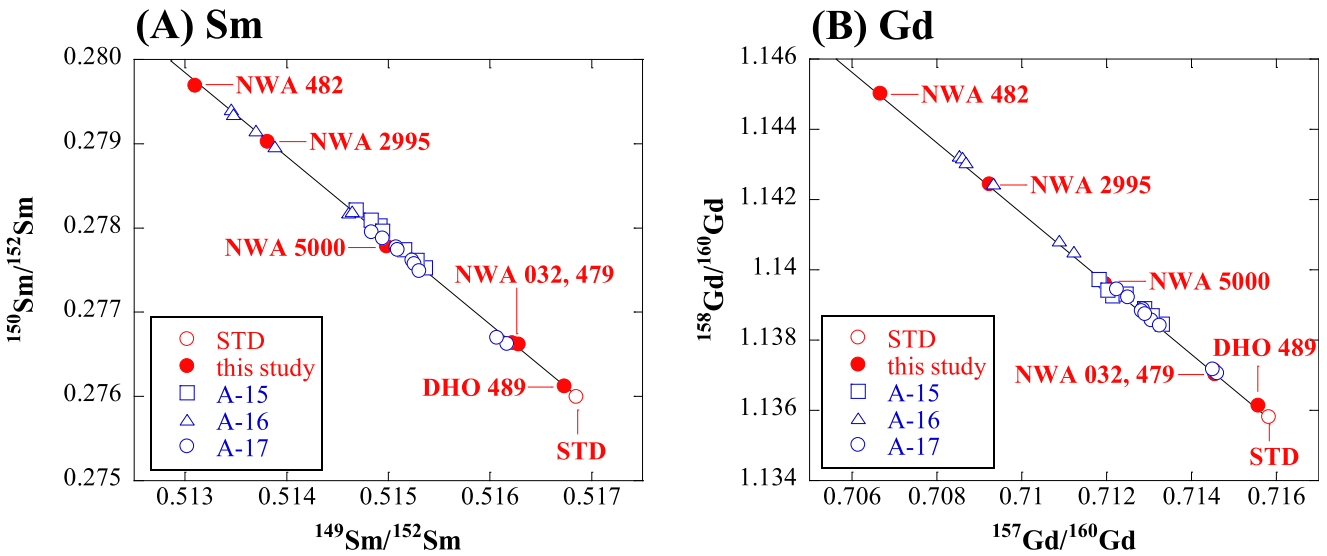

Figure 1. Correlation diagrams of isotopic shifts between (A) ^{149}Sm/^{152}Sm and ^{150}Sm/^{152}Sm, and (B) ^{157}Gd/^{160}Gd and ^{158}Gd/^{160}Gd. The reference data of lunar regoliths are cited from Hidaka et al. (2000) for A-15 and Hidaka & Yoneda (2007) for A-16 and A-17.

shifts of individual samples provide neutron fluences of (0.46–12.6) × 10^{16} n cm^{-2}. In particular, Gd and Sm isotopic shifts of NWA 482 are much larger than those of a lunar regolith 70002 from the Apollo-17 landing site, having the largest isotopic shifts among the Apollo lunar regolith samples, corresponding to cosmic-ray exposure ages of 700–1000 Ma in the lunar surface (Hidaka & Yoneda 2007).

3.2. Cosmogenic Radionuclides

The comparison of the data between cosmogenic radionuclides, ^{10}Be, ^{26}Al, ^{36}Cl, ^{41}Ca, and ^{53}Mn, provide useful information on the exposure conditions of individual meteorites, because the production rates of cosmogenic radionuclides on the Moon surface vary with depth. The depth profiles of cosmogenic ^{10}Be, ^{26}Al, ^{36}Cl, ^{41}Ca, and ^{53}Mn have been measured in the deep drill core at the Apollo-15 landing site (Nishiizumi et al. 1984a, 1984b). Since the lunar meteorites have been irradiated by two different exposure conditions, 2π exposure on the Moon before the ejection and 4π exposure in a space after the ejection from the Moon, the measured radioactivity of a cosmogenic radionuclide, A, is given as follows:

$$A = P_1(1 - e^{-\lambda T_1})e^{-\lambda(T_2+T_3)} + P_2(1 - e^{-\lambda T_2})e^{-\lambda T_3},$$

where P_1 is the production rate on the Moon (2π exposure), P_2 is the production rate in space (4π exposure), λ is the decay constant of the radionuclide, T_1 is the exposure age on the Moon, T_2 is the exposure age in space, and T_3 is the terrestrial age.

Assuming that all of the cosmogenic radionuclides were produced by a 4π exposure during the transit from the Moon to the Earth, there is a large difference of the estimated 4π exposure ages between ^{10}Be and ^{36}Cl of individual samples. This reveals that major amounts of the cosmogenic radionuclides of individual meteorites were produced as a 2π exposure on the Moon before the ejection. The production rates of the cosmogenic radionuclides, P_1, as a function of depth on the lunar surface, are required to determine a 2π exposure on the Moon. The measured activities of cosmogenic radionuclides from the Apollo-15 regolith core samples provide a depth-dependence (Nishiizumi et al. 1984a, 1984b), and can be used as a reference to determine the residence depth of individual lunar meteorites in a regolith. We estimated the depth level that lunar meteorites had resided in the regolith by comparison of the ^{10}Be and ^{36}Cl activities between individual meteorites and the Apollo-15 regolith core samples. Furthermore, the combination of the abundances of the cosmogenic radionuclides and isotopic data of neutron-captured products will make it possible to put some constraints into the following exposure conditions; (1) the depth of individual samples had resided on the Moon (shielding depth), and (2) the time of the samples had been irradiated by cosmic rays (2π exposure age). The depths of individual samples in regolith estimated from the combination of the abundances of long-lived cosmogenic nuclides are given in Table 4.

3.3. Neutron Energy Spectra

The isotopic shifts of ^{150}Sm/^{149}Sm and ^{158}Gd/^{157}Gd by neutron capture effects have the advantage to accumulate the cosmic-ray exposure records that the target had been experienced since the formation, because these parent nuclides and produced nuclides are all stable isotopes. Assuming that the samples had resided at the same depth in the regolith before ejection, individual residence time on the Moon was estimated. A variation in $\varepsilon_{Sm}/\varepsilon_{Gd}$ as a function of $\sum_{eff}$ is interpreted to be the result of differences in the neutron energy spectra (Lingenfelter et al. 1972). Furthermore, the combination of the isotopic shifts of ^{150}Sm/^{149}Sm and ^{158}Gd/^{157}Gd, defined as $\varepsilon_{Sm}/\varepsilon_{Gd}$ values, provides a measure of the energy spectrum,

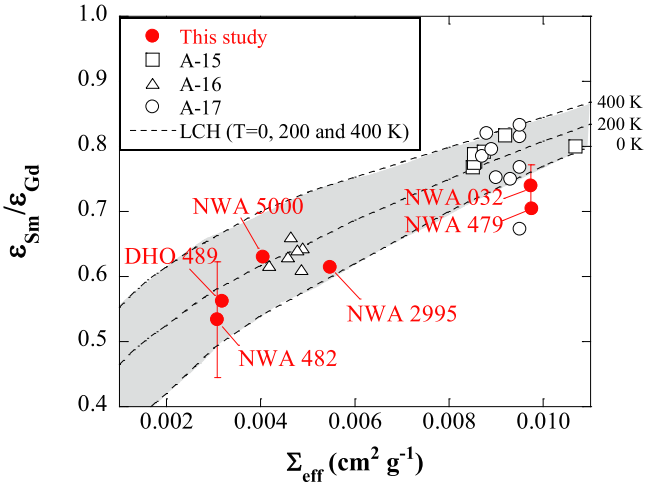

Figure 2. Correlation diagram between effective macroscopic neutron capture cross section ($\sum_{eff}$) and a parameter of neutron energy spectrum defined as $\varepsilon_{Sm}/\varepsilon_{Gd}$. The reference data of lunar regoliths are cited from Hidaka et al. (2000) for A-15 and Hidaka & Yoneda (2007) for A-16 and A-17. The shaded zone in the figure shows predicted values under the temperature between 0 and 400 K (Lingenfelter et al. 1972).

showing a thermalization degree of neutrons arising in a target material (Lingenfelter et al. 1972), because there is a difference in neutron capture resonance between ^{149}Sm (0.0973 eV) and ^{157}Gd (0.0314 eV), which can be effectively used to estimate the energy level of thermal neutrons. The $\varepsilon_{Sm}/\varepsilon_{Gd}$ values of individual samples are calculated as follows:

$$\frac{\varepsilon_{Sm}}{\varepsilon_{Gd}} = \frac{\dfrac{(^{150}Sm/^{149}Sm)_{sample} - (^{150}Sm/^{149}Sm)_{STD}}{1 + (^{150}Sm/^{149}Sm)_{sample}}}{\dfrac{(^{158}Gd/^{157}Gd)_{sample} - (^{158}Gd/^{157}Gd)_{STD}}{1 + (^{158}Gd/^{157}Gd)_{sample}}}.$$

The shape of neutron energy spectrum is dependent on the chemical compositions and temperature of the materials that are exposed to cosmic rays. From the viewpoint of neutron capture reactions, the chemical composition of the materials is often treated as a macroscopic cross section ($\sum_{eff}$) consisting of the summation of the neutron capture cross sections of major to minor constitution elements. The macroscopic cross section for individual samples are determined from the abundances of effective elements, Al, Ca, Fe, Mg, Si, Ti, Sm, Eu, and Gd. The variation of $\varepsilon_{Sm}/\varepsilon_{Gd}$ as a function of $\sum_{eff}$ is effective to consider the energy spectra of thermal neutrons arising in a material. The data of six lunar meteorites treated in this study are plotted in a diagram between $\varepsilon_{Sm}/\varepsilon_{Gd}$ and $\sum_{eff}$, as shown in Figure 2. For the calculation of the $\sum_{eff}$ values, the data of elemental abundances listed in Tables 1 and 2 were mainly used. The data of Si and Ti contents for all six meteorites and REE data for Dhofar 489 and NWA 032, that were not measured in this study, were cited from the previous studies (Daubar et al. 2002; Barrat et al. 2005; Korotev et al. 2006, 2009; Elardo et al. 2014; Nagurney et al. 2016). The parameters to characterize neutron capture reactions are listed in Table 5. For comparison of the data measured in this study, theoretical calculation data assuming the temperature at 0, 200, and 400 K (Lingenfelter et al. 1972), and previously measured data of three kinds of lunar regolith core samples from the landing sites of the Apollo mission 15, 16, and 17 (Hidaka & Yoneda 2007), were also given in the figure. Since all six meteorites had been resided in the lunar regolith at a certain depth (>200 g cm^{-2}) that is enough to lose the energy of arising neutrons down to the level of thermal neutron, it is expected that

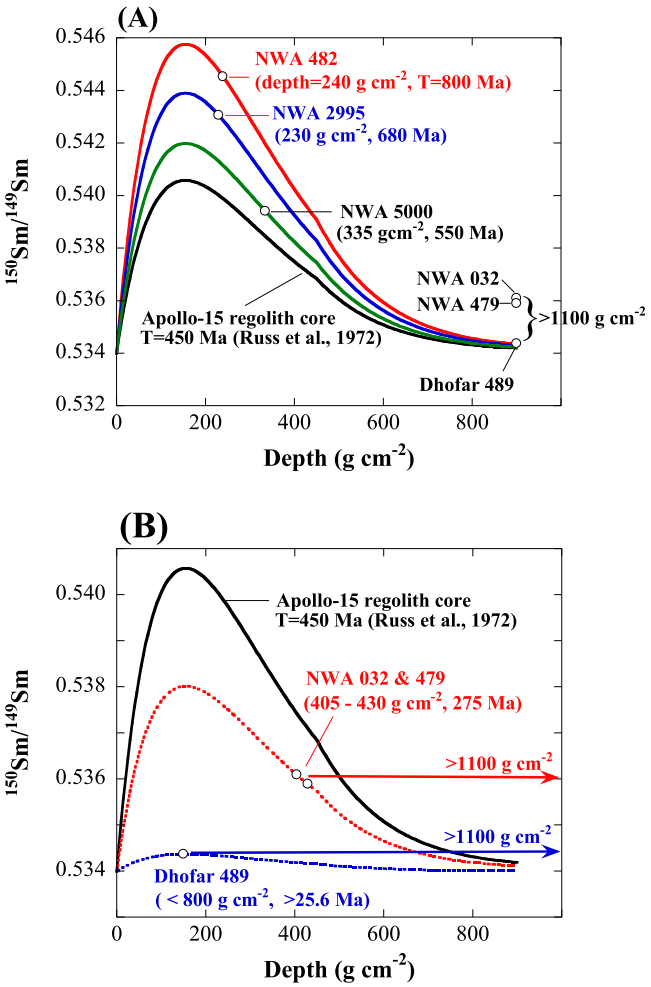

Figure 3. Fitting curves of the variation of $^{150}Sm/^{149}Sm$ isotopic shifts as a function of the depth (g cm^{-2}) on the lunar surface by (A) single-stage irradiation and (B) two-stage irradiation model of individual samples on the Moon. The curves are prepared to be adjusted at the data of burial depths and $^{150}Sm/^{149}Sm$ isotopic ratios for individual lunar meteorites. The burial depths are given by the combination of the abundances of measured cosmogenic nuclides (Table 3). The data for NWA 482, NWA 2995, and NWA 5000 are plotted on the fitting curves, but not for Dhofar 489, NWA 032, and NWA 479 in Figure 3(A). It is required for Dhofar 489, NWA 032, and NWA 479 to have been once irradiated at a shallower level than 800 g cm^{-2}, and then migrated into the deeper level over 1100 g cm^{-2} (see the text).

they were mostly affected by thermal neutrons. Judging from the energy spectra shown in Figure 2, neutrons of the six meteorites are well thermalized. However, strictly speaking, the chemical compositions of individual meteorites are not always similar to those in the regolith in which the meteorites had resided for a long time. The neutron energy is largely dependent upon the chemical compositions of the regolith where the individual meteorites had been buried, because the neutrons reduce their energy before reach at the meteorite fragments in the regolith. The neutrons arising in NWA 032 and NWA 479 are more well thermalized than those in other species. This suggests that NWA 032 and NWA 479 had been irradiated by cosmic rays in deep locations that are enough distance for the arising neutrons to lose their energy down to the level of thermal neutron.

3.4. Burial Depth in the Regolith on the Moon

The depth profile of the isotopic variation of $^{150}Sm/^{149}Sm$ has been measured in the Apollo-15 (A-15) regolith core (Russ et al. 1972; Hidaka et al. 2000). The results reveal that the neutron fluence (n cm^{-2}) of the A-15 regolith has a function of the depth, showing a smooth curve with a maximum peak at the depth of 155 g cm,$^{-2}$ which is produced by accumulation of cosmic-ray irradiation on the A-15 slab for 450 Ma (Russ et al. 1972). The neutron fluence curve of the A-15 core can be used as a reference to determine the residence time of individual lunar meteorites at a certain depth in a regolith.

Figure 3 shows fitting curves of the $^{150}Sm/^{149}Sm$ isotopic variations of six individual lunar meteorites in the A-15 regolith core. The $^{150}Sm/^{149}Sm$ isotopic variations corresponding to the neutron capture rates can be considered as a function of depth beneath the lunar surface (Lingenfelter et al. 1972). Providing no geometric disturbance in the regolith by any bombardments on the lunar surface, the fitting curves vary with the duration of cosmic-ray irradiation. The curves are adjusted at the burial depths of individual meteorites that were determined from the measured abundances of cosmogenic radionuclides given in Table 3. As shown in Figure 3, all of the meteorites had resided at a deeper level than 200 g cm^{-2}. The time variation of the curves are distinct in the depth level shallower than 800 g cm^{-2}. In the deeper region over 800 g cm^{-2} in the lunar regolith, it is difficult to distinguish a difference in the time variation of $^{150}Sm/^{149}Sm$ isotopic shift in the current analytical precision. The burial depths of NWA 482, NWA 2995, and NWA 5000, having large Sm isotopic shifts, are estimated to be 240, 230, and 335 g cm^{-2}, respectively (see Table 3). Assuming that the individual meteorites had resided at their original depths without geometrical disturbance during the cosmic-ray irradiation on the Moon, the exposure ages of NWA 482, NWA 2995, and NWA 5000 on the Moon are calculated to be 800 Ma, 680 Ma, and 550 Ma, respectively, from the comparison with the data of the fitting curve of A-15 core having the exposure age of 450 Ma, as shown in Figure 3(A).

On the other hand, the depth levels of Dhofar 489, NWA 032, and NWA 479 were estimated to be deeper than 1100 g cm^{-2} from the abundances of cosmogenic nuclides in Table 3, which are inconsistent with those of $^{150}Sm/^{149}Sm$ isotopic shifts, showing small but significant variations. The $^{150}Sm/^{149}Sm$ isotopic variations of three meteorites, Dhofar 489, NWA 032, and NWA 479, are clearly resolved from that of the non-irradiated materials ($^{150}Sm/^{149}Sm = 0.533991$, given as STD in Table 5) within the analytical precision. It is reasonable to consider that these three species had once resided at shallower positions at the depth less than 800 g cm^{-2}, where the cosmic rays had interacted effectively before they had migrated at the deeper level over 1100 g cm^{-2}, where most of the cosmic rays had been shielded. In the first stage of this two-stage 2π irradiation model, Dhofar 489 had been irradiated by the cosmic rays at least for 25.6 Ma, estimated from the maximum peaks at the depth of 155 g cm^{-2} in the fitting curve shown in Figure 3(B). As shown in the same figure, the first stage of NWA 032 and NWA 479 having 2π an exposure age of 275 Ma (Fernandes et al. 2009; Elardo et al. 2014) can be explained by the irradiation at the depth of 405–430 g cm^{-2} .

4. Conclusions

A large discrepancy of the estimated exposure ages between cosmogenic radionuclides of six lunar meteorites indicates that major amounts of the cosmogenic radionuclides were produced as 2π exposure on the Moon before the ejection. Assuming the

production rates of the long-lived cosmogenic radionuclides as a function of depth on the lunar surface based on the measurement of those in the A-15 drill core, the depth location of individual samples in the lunar regolith can be determined.

The isotopic shifts of ^{150}Sm/^{149}Sm and ^{158}Gd/^{157}Gd due to neutron capture clearly preserve the 2π exposure records on the Moon. Furthermore, the neutron energy spectra given by the combination of the Sm and Gd isotopic shifts, εSm/εGd, show that the arising neutrons in six meteorites were well thermalized on the Moon, which is consistent with the depth information given by the cosmogenic radionuclides. All six meteorites had been resided in the lunar regolith at a certain depth ($>200\,\mathrm{g\,cm^{-2}}$) that is enough to lose the energy of arising neutrons down to the level of thermal neutron. In particular, the combined data of cosmogenic nuclides and Sm–Gd isotopic shifts suggest that three meteorites, Dhofar 489, NWA 032, and NWA 479, had been once irradiated at a shallower depth ($<800\,\mathrm{g\,cm^{-2}}$) before they had migrated into deeper levels ($>1100\,\mathrm{g\,cm^{-2}}$) until the release from the Moon.

This study was financially supported by a Grant-in-Aid for Scientific Research from the Japan Society for the Promotion of Science (to H.H., No. 26247095).

References

Barrat, J. A., Chaussidon, M., Bohin, M., et al. 2005, GeCoA, 69, 5597
Borg, L. E., Gaffney, A. M., Shearer, C. K., et al. 2009, GeCoA, 73, 3963
Carpenter, P. K., Hahn, T. M., Korotev, R. A., et al. 2017, LPSC, 48, 2607
Connolly, H. C., Smith, C., Benedix, G., et al. 2008, M&PS, 43, 571
Daubar, I. J., Kring, D. A., Swindle, T. D., & Jull, A. J. T. 2002, M&PS, 37, 1797
Elardo, S. M., Shearer, C. K., Fagan, A. L., et al. 2014, M&PS, 49, 261
Fernandes, V. A., Burgess, R., & Morris, A. 2009, M&PS, 44, 805
Hidaka, H., Ebihara, M., & Shima, M. 1995, AnaCh, 67, 1437
Hidaka, H., Ebihara, M., & Yoneda, S. 2000, M&PS, 35, 581
Hidaka, H., & Yoneda, S. 2007, GeCoA, 71, 1074
Hidaka, H., & Yoneda, S. 2013, M&PSA, 76, 5042
Hidaka, H., & Yoneda, S. 2014, ApJ, 786, 138
Joy, K. H., & Arai, T. 2013, A&G, 54, 428
Korotev, R. L. 2005, ChEG, 65, 297
Korotev, R. L., Zeigler, R. A., & Jolliff, B. L. 2006, GeCoA, 70, 5935
Korotev, R. L., Zeigler, R. A., Jolliff, B. L., Irving, A. J., & Bunch, T. E. 2009, M&PS, 44, 1287
Lingenfelter, R. E., Canfield, E. H., & Hampel, V. E. 1972, E&PSL, 16, 355
Mercer, C. N., Treiman, A. H., & Joy, K. H. 2013, M&PS, 48, 289
Nagurney, A. B., Treiman, A. H., & Spudis, P. D. 2016, LPSC, 47, 1103
Nishiizumi, K., & Caffee, M. W. 2001, LPSC, 32, 2101
Nishiizumi, K., Caffee, M. W., Jull, A. J. T., & Reedy, R. C. 1996, M&PS, 31, 893
Nishiizumi, K., Caffee, M. W., Vogel, N., et al. 2009, LPSC, 40, 1476
Nishiizumi, K., Elmore, D., Ma, X. Z., & Arnold, J. R. 1984a, E&PSL, 70, 157
Nishiizumi, K., Hillegonds, D. J., McHargue, L. R., & Jull, A. J. T. 2004, LPSC, 35, 1130
Nishiizumi, K., Klein, J., Middleton, R., & Arnold, J. R. 1984b, E&PSL, 70, 164
Russ, G. P., Burnett, D. S., & Wasserburg, G. J. 1972, E&PSL, 15, 172
Takeda, H., Arai, T., Yamaguchi, A., Otsuki, M., & Ishii, T. 2007, LPSC, 38, 1607
Weisberg, M. K., Smith, C., Benedix, G., et al. 2008, M&PS, 43, 1551
Weisberg, M. K., Smith, C., Benedix, G., et al. 2009, M&PS, 44, 1355
Welten, K. C., Nishiizumi, K., Caffee, M. W., & Schultz, L. 2001, M&PSA, 36, 223
Welten, K. C., Owens, T. L., DePaolo, D. J., & Nishiizumi, K. 2013, LPSC, 44, 2933